ISSN (e): 2250 – 3005 || Volume, 08 || Issue, 2|| February – 2018 ||
International Journal of Computational Engineering Research (IJCER)

# An Overview of Extraction and Evaluation of Optical Phase Distribution by the Use of a Wavelet Based Algorithm

**Saad Cheffah, Pr. Mohamed Afifi**
*LTI laboratory, Faculty of sciences Ben M'sik, Hassan II University, Casablanca, Morocco*
*Corresponding author: Saad Cheffah*

**ABSTRACT**
In this paper, we present an overview of the direct extraction of phase from fringe pattern by the use of a wavelet transform algorithm based on the Morlet mother wavelet function. Numerical simulations are presented, to demonstrate the ability of our method to provide, with a good accuracy, phase distribution from a single image without the unwrapping step. The numerical results are compared to those obtained previously by phase shifting technique.
**Keywords:** Optical metrology, phase extraction, wavelet transform, fringe pattern analysis.

## I. INTRODUCTION

Optical interferometry techniques are increasingly employed in various sciences and engineering applications to compute several physical magnitudes which are codified as the phase of a periodic intensity profiles, such as micro-displacements and micro-deformations in several scientific and industrial applications [1,2]. These nondestructive methods are based on the measurement of small variation of the optical path with the interference phenomena. Thus the development of effective and sophisticated phase extraction algorithms is continuously needed [3-6]. In this context the wavelet concept is very useful to analyze non-stationary or transient signals [7,8]. A good review of wavelet theory has been published by Daubechies [9].
This article presents an overview of a phase evaluation method, based on Morlet wavelet algorithm, which extracts the phase gradient from a single fringe pattern directly. The spatial phase distribution being obtained by integration of the gradient, the complex phase unwrapping step is no longer needed [10]. Thus the use of a single image can lead to the phase distribution of dynamic processes, while the unwrapping step, which provides a continuous phase distribution over its definition domain, implies several difficulties and requires sophisticated algorithms.
The paper first presents an introduction of the continuous wavelet transform. We present in paragraph 2 the wavelet phase analysis method and we propose a discussion on the Morlet wavelet, particularly on the choice of space and frequency resolutions. In paragraph 3 we describe the process of phase extraction by the wavelet technique.
Finally, results of numerical simulations are presented in paragraph 4, and demonstrate the ability of the presented method to give the phase distribution with good accuracy.

## II. WAVELET ANALYSIS

Wavelets offer a powerful method to quantify how energy is spatially distributed at multiple scales [11]. Wavelets transform a signal into a series of coefficients having discrete energies. The original signal is completely specified by these coefficients and the analyzing wavelet. Wavelet analysis is similar to the Fourier transform (FT). The FT is useful for the analysis of stationary signals but is less suitable for non-stationary signals.

### 2.1. Wavelet transform

In the Continuous Wavelet Transform CWT, the coefficient $W(s,\xi)$ of two variables, scale s and shift $\xi$ , is given by

$$W(s,\xi) = \langle f \,|\Psi_{s,\xi}\rangle = \frac{1}{\sqrt{s}}\int_{-\infty}^{+\infty} f(x)\left(\Psi\left(\frac{x-\xi}{s}\right)\right)^{*} dx \qquad (1)$$

Where * denotes complex conjugation, *f(x)* is the signal to be analyzed, $\Psi_{s,\xi}(x)$ is the analyzing wavelet, $s > 0$ is the scale parameter related to the frequency concept, and $\xi$ is the shift parameter related to position.
The *W*(s,ξ) coefficients quantify the similitude between the signal *f(x)* and the wavelet $\Psi_{s,\xi}(x)$. For a given scale at a position $\xi$, the magnitude of this resemblance is given by the modulus of *W*(s,ξ). The *W*(s,ξ) is also regarded as coordinates of the signal projected in the wavelet basis formed by $\Psi_{s,\xi}(x)$ set.
From the admissible and localized mother wavelet $\Psi(x)$, the analyzing wavelet $\Psi_{s,\xi}(x)$ is obtained by shifting and scaling :

$$\Psi_{s,\xi}(x) = \frac{1}{\sqrt{s}}\Psi\left(\frac{x-\xi}{s}\right) \tag{2}$$

Admissibility and localization conditions are obtained when the analyzing wavelet has respectively a zero mean and a zero value outside a given interval in both space and frequency domains.
The wavelet transform can be expressed, using the Parseval identity, as

$$W(s,\xi) = \frac{1}{2\pi}\langle \hat{f} \,|\hat{\Psi}_{s,\xi}\rangle = \frac{\sqrt{s}}{2\pi}\int_{-\infty}^{+\infty}\hat{f}(k)\left(\hat{\Psi}(sk)\right)^{*} e^{i\xi k}\, dk \tag{3}$$

Where $\hat{f}$ and $\hat{\Psi}$ are, respectively, the FT of the signal and the mother wavelet, and *k* is the conjugate of *x* and denotes the angular frequency.
If the inverse wavelet transform exists, the original signal can be reconstructed by:

$$f(x) = \frac{1}{C_\Psi} = \int_0^{+\infty}\int_{-\infty}^{+\infty} W(s,\xi)\Psi_{s,\xi}(x)\frac{ds d\xi}{s^2} \tag{4}$$

Where

$$C_\Psi = \int_{-\infty}^{+\infty}\frac{\left|\hat{\Psi}(k)\right|^2}{k}\, dk \tag{5}$$

This reconstruction of the signal is possible when $C_\Psi$ has a finite value.

**2.2. Paul wavelet**

The appropriate choice of the mother wavelet *Ψ(x)*, characterized by its shape, is important for specific applications. For phase evaluation problems, several well localized mother wavelet, like ‘‘Morlet’’ [12,13], ‘‘Hermitian’’ [14,15] or ‘‘Paul’’ [16] wavelet could be chosen. In the present work, our purpose is to use the second order of Paul wavelet which is formulated by

$$\Psi(x) = \frac{2^n(1-ix)^{-(n+1)}}{2\pi\sqrt{(2n)!/2}} \tag{6}$$

where *n* is the order of the Paul wavelet. Its FT is

$$\hat{\Psi}(k) = \frac{2^n}{\sqrt{n(2n-1)!}}k^n e^{-x}H(k) \tag{7}$$

where *H* is the Heaviside distribution.

The analyzing wavelet, obtained by shifting and scaling the Paul wavelet is

$$\Psi_{s,\xi}(x) = \frac{1}{\sqrt{s}}\Psi\left(\frac{x-\xi}{s}\right) = \frac{1}{\sqrt{s}}\frac{2^n(1-i\frac{x-\xi}{s})^{-(n+1)}}{2\pi\sqrt{(2n)!/2}} \tag{8}$$

In space domain, the center of the analyzing wavelet is given by

$$x_c = = \frac{\int_{-\infty}^{+\infty} x\left|\Psi_{s,\xi}(x)\right|^2 dx}{\int_{-\infty}^{+\infty}\left|\Psi_{s,\xi}(x)\right|^2 dx} = \xi \tag{9}$$

and the associated variance is

$$(\Delta x)^2 = \frac{\int_{-\infty}^{+\infty}(x-x_c)^2\left|\Psi_{s,\xi}(x)\right|^2 dx}{\int_{-\infty}^{+\infty}\left|\Psi_{s,\xi}(x)\right|^2 dx} = \frac{s^2}{2n-1} \quad \textbf{(10)}$$

then

$$\Delta x = \frac{s}{\sqrt{2n-1}} \quad \textbf{(11)}$$

we note that the resolution $\Delta x$ in the space domain depends on the used order and particularly the scale *s*. Information about the structure of the signal is concentrated in the interval $[x_c - \Delta x, x_c + \Delta x]$.

Similarly, in frequency domain, the center of the analyzing wavelet is given by

$$k_c = = \frac{\int_{-\infty}^{+\infty} k\left|\hat{\Psi}_{s,\xi}(k)\right|^2 dk}{\int_{-\infty}^{+\infty}\left|\hat{\Psi}_{s,\xi}(k)\right|^2 dk} = \frac{2n+1}{2s} \quad \textbf{(12)}$$

and the associated variance is

$$(\Delta k)^2 = \frac{\int_{-\infty}^{+\infty}(k-k_c)^2\left|\hat{\Psi}_{s,\xi}(k)\right|^2 dk}{\int_{-\infty}^{+\infty}\left|\hat{\Psi}_{s,\xi}(k)\right|^2 dk} = \frac{2n+1}{4s^2} \quad \textbf{(13)}$$

then

$$\Delta k = \frac{\sqrt{2n+1}}{2s} \quad \textbf{(14)}$$

we note that frequency resolution $\Delta k$, depends on the used order and particularly the scale *s*. In this case, the most important information about the structure of the signal is concentrated in the interval $[k_c - \Delta k, k_c + \Delta k]$.

Paul mother wavelet and its Fourier Transform FT are presented in Figure 1. In Figure 1a, we plot the real part (solid line) and imaginary part (dashed line) for the second order Paul wavelet (n = 2). In Figure 1b, we plot the Paul wavelet FT.

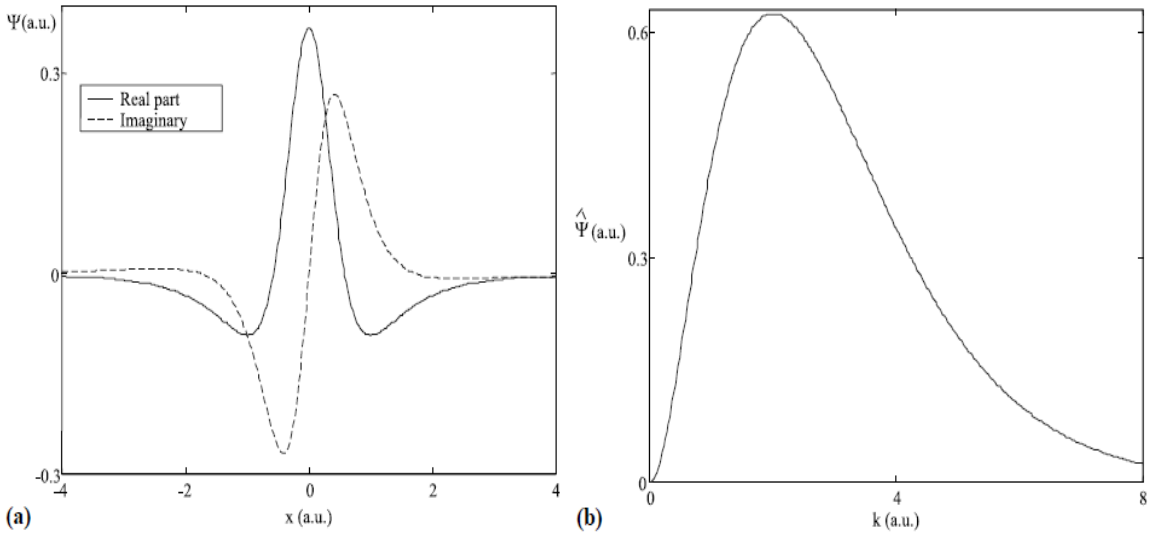


***Figure 1. (a) Paul wavelet (n = 2); (b) Fourier Transform of Paul wavelet.***

## III. WAVELET PHASE EXTRACTION

There are many techniques for extracting phase distributions from two-dimensional fringe patterns [4]. The fringe patterns, derived from two-beam interferometers, can be mathematically formulated by the sinusoidal dependence of the intensity on the spatial coordinates *(x,y)* of the image plane

$$I(x,y) = I_0(x,y)[1 + V(x,y)cos(my + \varphi(x,y))] \quad \textbf{(15)}$$

where $I_0$ is the bias intensity, $V$ the visibility or fringe contrast and $\varphi$ the optical phase (argument of the sinusoidal dependence). The $my$ added phase to the phase of interest is known as the phase modulated carrier. This spatial carrier must respect the following condition:

$$m > \left|\frac{\partial\varphi}{\partial y}\right|_{max} \quad \textbf{(16)}$$

The one-dimensional wavelet transform of the fringe pattern intensity, in the $y$ direction, is given by

$$W(x,s,\xi) = \frac{1}{\sqrt{s}}\int_{-\infty}^{+\infty} I_0(x,y)[1 + V(x,y)cos(my + \varphi(x,y))]\left(\Psi\left(\frac{y-\xi}{s}\right)\right)^* dy \quad \textbf{(17)}$$

Exploiting the localization property of the wavelet, the development of the phase of interest $\varphi$ on Taylor series near the central value $\xi$, allowed us to write

$$\varphi(x,y) = \varphi(x,\xi) + (y-\xi).\frac{\partial\varphi}{\partial y}(x,\xi) + \frac{1}{2}(y-\xi)^2.\frac{\partial^2\varphi}{\partial y^2}(x,\xi) + \cdots \quad \textbf{(18)}$$

Assuming a slow variation of the intensity bias $I_0$ and the visibility $V$, which is convenient in usual cases, and owing the localization of the wavelet, we can neglect the higher order of $(y-\xi)$ with respect to the phase-modulated carrier. With these considerations, the wavelet transform becomes

$$W(x,s,\xi) = \frac{I_0(x,\xi)V(x,\xi)}{\sqrt{s}}\int_{-\infty}^{+\infty} cos[my + \varphi(x,\xi) + (y-\xi).\frac{\partial\varphi}{\partial y}(x,\xi)].\left(\Psi\left(\frac{y-\xi}{s}\right)\right)^* dy \quad \textbf{(19)}$$

and the Parseval identity leads to

$$W(x,s,\xi) = \frac{\sqrt{s}}{2\pi}\int_{-\infty}^{+\infty} \hat{I}_a(x,k)\left(\widehat{\Psi}(sk)\right)^* e^{i\xi k}\,dk \quad \textbf{(20)}$$

where

$$\hat{I}_a(x,k) = I_0(x,\xi)V(x,\xi)\pi h(x,\xi) \quad \textbf{(21)}$$

with

$$h(x,\xi) = \delta(k-m_1).exp\left[i\left(\varphi(x,\xi) - \xi\frac{\partial\varphi}{\partial y}(x,\xi)\right)\right] + \delta(k+m_1).exp\left[-i\left(\varphi(x,\xi) - \xi\frac{\partial\varphi}{\partial y}(x,\xi)\right)\right] \quad \textbf{(22)}$$

and

$$m_1 = m + \frac{\partial\varphi}{\partial y}(x,\xi) \quad \textbf{(23)}$$

finally, the wavelet transform becomes

$$W(x,s,\xi) = \frac{I_0(x,\xi)V(x,\xi)\sqrt{s}}{2}\left[\left(\widehat{\Psi}(sm_1)\right)^* e^{i(\xi m+\varphi(x,\xi))} + \left(\widehat{\Psi}(-sm_1)\right)^* e^{-i(\xi m+\varphi(x,\xi))}\right] \quad \textbf{(24)}$$

by introducing Paul mother wavelet, we get

$$W(x,s,\xi) = \frac{I_0(x,\xi)V(x,\xi)s^{n+1/2}.m_1^n exp(-sm_1)}{(2n)!}\, e^{i(\xi m+\varphi(x,\xi))} \quad \textbf{(25)}$$

and its modulus is given by

$$|W(x,s,\xi)| = \left(\frac{I_0(x,\xi)V(x,\xi)m_1^n}{(2n)!}\right) s^{n+1/2}exp(-sm_1) \quad \textbf{(26)}$$

the extremum scale noted *S* is then given by

$$S(x,\xi) = \frac{2n+1}{2m_1} \tag{27}$$

Equations (23) and (27) then give the phase gradient by

$$\frac{\partial \varphi}{\partial y}(x,\xi) = \frac{2n+1}{2S(x,\xi)} - m \tag{28}$$

This leads to the phase by integration of the gradient. Moreover, for determining the phase distribution of two dimensional fringe pattern, we proceed as follows: for each row of the image, we extend the fringe pattern at its left-and right-hand edges, using zero padding method. This step is necessary to avoid discontinuities and hence spurious, large values of the CWT at the edges of the data.

## IV. SIMULATION RESULTS

In our numerical simulation, we used the Paul wavelet as a mother wavelet to verify the ability of the wavelet technique to determinate the phase with a quite good accuracy. The simulation consists in generating numerically a fringe pattern of a given phase distribution, retrieving this phase distribution by the wavelet method and comparing to the results obtained by phase shifting technique. The test phase function used is

$$\varphi(x,y) = 0.0005((x-256)^2 + (y-256)^2) \tag{29}$$

and the intensity distribution of fringe pattern is

$$I(x,y) = 1 + 0.5\cos(\varphi(x,y) + my) \tag{30}$$

where $m$ = 1.28 rad/pixel is the modulation carrier (the maximum gradient of the phase $\varphi$ is 0.26 rad/ pixel).

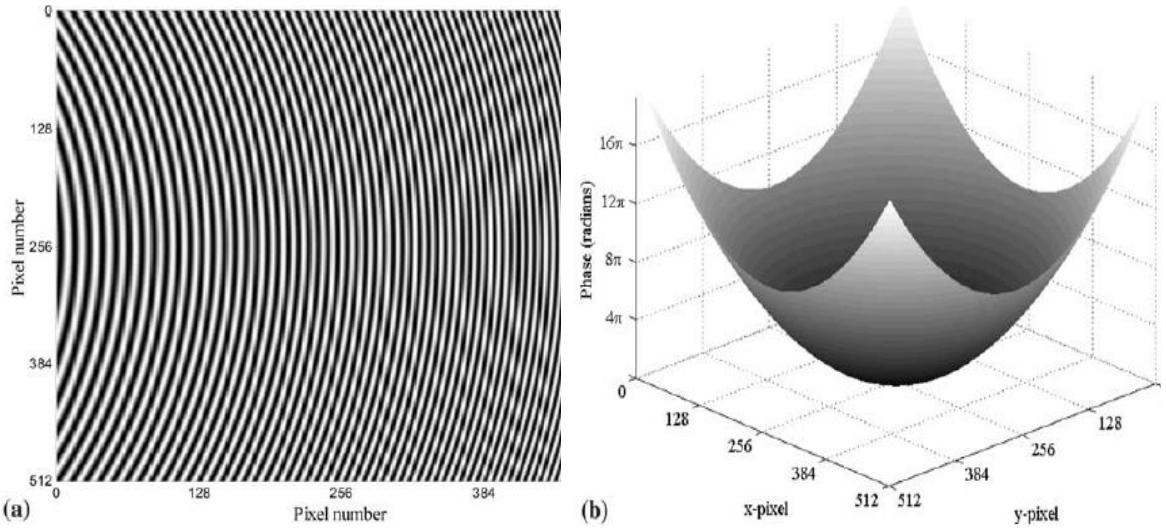


***Figure 2. (a) Simulated fringe pattern; (b) phase distribution extracted by wavelet method.***

The result of simulation is illustrated in Figure 2, where the test fringe pattern is depicted in Figure 2a while the retrieved phase distribution is plotted in Figure 2b. The phase distribution simulation is computed by MATLAB software. The phase accuracy is in the same order than the one obtained previously, by phase shifting algorithm [17].

## V. CONCLUSION

In this paper we present an overview of the use of wavelet transform and especially Paul wavelet, to extract phase distribution. Numerical simulations obtained by the use of the method presented here, are in excellent agreement with those produced by phase shifting methods. It is worth noting that this method gives the phase distribution with a single image and without unwrapping, while most phase evaluation methods, requires unwrapping phase over its definition domain, in the manner to provide a continuous phase distribution, but more sophisticated phase unwrapping algorithms are needed to overcome the difficulties involved in such process.

## REFERENCES

[1]. D.C. Williams, Optical methods in engineering metrology. Chapman and Hall. First edition, 1993.
[2]. S. Cheffah et al. Impact of Soft Oxide Breakdown on the functionality of a 40nm SRAM memory. In Proc. IEEE International Reliability Physics Symposium, pages IRPS11-704,705. IEEE IRPS, 2011.
[3]. A. H. Mazinan and A. Esmaeili. An algorithm for extracting the phase of the fringe patterns with its applications to three-dimensional imaging through FPGA based implementation. In Proc. IEEE International Conference on Industrial Informatics and Computer Systems. IEEE CIICS, 2016.
[4]. B. V. Dorrio, and L. L. Fernandez, Phase-evaluation methods in whole-field optical measurement techniques, Meas. Sci. Technol. 10, 33-55, 1999.
[5]. M. Afifi, A. Fassi-Fihri, M. Marjane, K. Nassim, M. Sidki, S. Rachafi, Paul wavelet based algorithm for optical phase distribution evaluation, Opt. Commun. 211, 47–51, 2002.
[6]. L.R. Watkins, S.M. Tau, T.H. Barnes, Opt. Lett. 24 (13) 905, 1999.
[7]. I. Daubechies, IEEE Trans. Inform. Theory 36, 961, 1990.
[8]. M. Friesch, H. Messer, IEEE Trans. Inform. Theory 38, 892, 1992.
[9]. I. Daubechies, Ten Lectures on Wavelets, Society for Industrial and Applied Mathematics, Philadelphia, PA, 1992.
[10]. T.R. Judge, P.J. Bryanston-Cross, A review of phase unwrapping techniques in fringe analysis, Opt. Laser Eng. 21 199-239, 1994.
[11]. G. Kaiser, A Friendly Guide to Wavelets, Birkhauser, Boston, MA, 1994.
[12]. L.R. Watkins, S.M. Tau, T.H. Barnes, Opt. Lett. 24 (13) (1999) 905.
[13]. M Bahich, M Afifi, EM Barj, A numerical spatial carrier for single fringe pattern analysis algorithm. Optic 122 (2011) 1821-1824.
[14]. H. Szu, C. Hsu, L. Sa, W. Li, in: Wavelet Applications IV, Proc. SPIE 3078, 96,1997.
[15]. S. Noel, Y. Gohel, in: Wavelet Applications IV, Proc. SPIE 3078, 374,1997.
[16]. C. Torrence, G.P. Compo, Bull. Am. Meteorol. Soc. 79, 61, 1998.
[17]. M. Afifi, K. Nassim, S. Rachafi, Opt. Commun. 197 (2001) 37.

Saad Cheffah "An Overview of Extraction and Evaluation of Optical Phase Distribution by the Use of a Wavelet Based Algorithm" International Journal of Computational Engineering Research (IJCER), vol. 08, no. 02, 2018, pp. 37–42.